Clinical Research Article

Aberrant Splicing of *SDHC* in Families With Unexplained Succinate Dehydrogenase-Deficient Paragangliomas

Sunita M.C. De Sousa,[1,2,3,4] John Toubia,[5] Tristan S.E. Hardy,[6,7] Jinghua Feng,[5,8] Paul Wang,[5] Andreas W. Schreiber,[5,8,9] Joel Geoghegan,[5] Rachel Hall,[10] Lesley Rawlings,[6] Michael Buckland,[11,12] Catherine Luxford,[13] Talia Novos,[13] Roderick J. Clifton-Bligh,[13] Nicola K. Poplawski,[3,4] Hamish S. Scott,[2,4,5,8,9,*] and David J. Torpy[1,4,*]

[1]Endocrine and Metabolic Unit, Royal Adelaide Hospital, Adelaide 5000, Australia; [2]Department of Genetics and Molecular Pathology, Centre for Cancer Biology, an SA Pathology and University of South Australia alliance, Adelaide 5000, Australia; [3]Adult Genetics Unit, Royal Adelaide Hospital, Adelaide 5000, Australia; [4]School of Medicine, University of Adelaide, Adelaide 5000, Australia; [5]ACRF Cancer Genomics Facility, Centre for Cancer Biology, SA Pathology, Adelaide 5000, Australia; [6]SA Pathology, Adelaide 5000, Australia; [7]Repromed, Dulwich 5065, Australia; [8]School of Pharmacy and Medical Sciences, University of South Australia, Adelaide 5000, Australia; [9]School of Biological Sciences, University of Adelaide, Adelaide 5000, Australia; [10]SA Pathology, Flinders Medical Centre, Bedford Park 5042, Australia; [11]Department of Neuropathology, Royal Prince Alfred Hospital, Camperdown 2050, Australia; [12]School of Medical Sciences, University of Sydney, Sydney 2000, Australia; and [13]Cancer Genetics, Kolling Institute of Medical Research, Royal North Shore Hospital, Sydney 2000, Australia

ORCiD numbers: 0000-0003-0127-6482 (S.M.C. De Sousa); 0000-0002-5878-0340 (T.S.E. Hardy); 0000-0003-4755-6471 (M. Buckland); 0000-0002-5813-631X (H. S. Scott).

*H.S.S. and D.J.T. contributed equally to this work.

Abstract

Context: Germline mutations in the succinate dehydrogenase genes (*SDHA/B/C/D*, *SDHAF2*—collectively, "*SDHx*") have been implicated in paraganglioma (PGL), renal cell carcinoma (RCC), gastrointestinal stromal tumor (GIST), and pituitary adenoma (PA). Negative SDHB tumor staining is indicative of SDH-deficient tumors, usually reflecting an underlying germline *SDHx* mutation. However, approximately 20% of individuals with SDH-deficient tumors lack an identifiable germline *SDHx* mutation.

Methods: We performed whole-exome sequencing (WES) of germline and tumor DNA followed by Sanger sequencing validation, transcriptome analysis, metabolomic studies, and haplotype analysis in 2 Italian-Australian families with SDH-deficient PGLs and various neoplasms, including RCC, GIST, and PA.

Results: Germline WES revealed a novel *SDHC* intronic variant, which had been missed during previous routine testing, in 4 affected siblings of the index family. Transcriptome analysis demonstrated aberrant *SDHC* splicing, with the retained intronic segment introducing a premature stop codon. WES of available tumors in this family showed chromosome 1 deletion with loss of wild-type *SDHC* in a PGL and a somatic gain-of-function *KIT* mutation in a GIST. The *SDHC* intronic variant identified was subsequently detected in the second family, with haplotype analysis indicating a founder effect.

Conclusions: This is the deepest intronic variant to be reported among the *SDHx* genes. Intronic variants beyond the limits of standard gene sequencing analysis should be considered in patients with SDH-deficient tumors but negative genetic test results.

Key Words: paraganglioma, succinate dehydrogenase, *SDHC*, intronic mutation, whole-exome sequencing

Involved in both the Krebs cycle and mitochondrial respiratory chain, succinate dehydrogenase (SDH) is a heterotetramer protein complex encoded by the *SDHA*, *SDHB*, *SDHC*, and *SDHD* genes [1]. Together with *SDHAF2*, which allows flavination and functioning of the SDHA subunit [2], these genes are collectively referred to as the "*SDHx*" genes. Loss-of-function *SDHx* variants inactivate SDH, leading to reactive oxygen species and succinate accumulation; the combined effect is inhibition of prolyl hydroxylases, resulting in decreased hydroxylation (inactivation) of hypoxia-inducible factor α, angiogenesis, cellular proliferation, and eventual tumorigenesis [1, 3, 4].

Consistent with the tumor-suppressor gene model, *SDHx* tumor syndromes demonstrate autosomal dominant inheritance due to heterozygous germline mutations, and variable penetrance and expressivity related to the timing of the somatic second hit, which is most commonly loss of heterozygosity, followed by somatic mutations, and, rarely, epigenetic inactivation [1, 3, 5]. SDHB tumor immunohistochemistry (IHC) is used to identify SDH-deficient tumors, with loss of any component of the SDH complex resulting in negative SDHB staining [2, 6-8]. In addition, the inactivation of SDH produces an excess of succinate, which can be directly assessed in tumor specimens, with high succinate:fumarate ratios indicative of SDH deficiency [2, 9].

Pheochromocytomas and paragangliomas (collectively, PPGLs) are the archetypal SDH-deficient tumor. Paragangliomas (PGLs) may involve any of the parasympathetic or sympathetic ganglia [3], making surveillance onerous and emphasizing the value of identifying causative mutations in PPGL kindreds to restrict follow-up to proven mutation carriers. PPGLs are regarded as the most heritable tumors in humans [5], with germline mutations identified in more than 30% of all-comers and 13% to 24% of sporadic cases [10-14]. Given the high mutation probability for most patients, and the clinical utility for patients and their families [15], genetic testing should be offered to all patients with PPGL [10]. Single/staged gene sequencing by direct sequencing has been supplanted by next-generation sequencing (NGS), addressing the marked genetic heterogeneity in PPGL with more than 15 genes implicated to date [5]. The role of SDH deficiency in PPGL is underscored by *SDHx* mutations accounting for approximately half of all heritable PPGL syndromes [2, 10]. SDH deficiency has also been implicated in smaller proportions of gastrointestinal stromal tumor (GIST), renal cell carcinoma (RCC), and pituitary adenoma (PA) [3]. These tumor types may coexist within individuals; however, no individuals or families have been reported to exhibit all 4 SDH-related tumors. Syndromes have been named according to specific tumor combinations: Carney triad for PGL, GIST, and pulmonary chondroma [16]; Carney-Stratakis dyad for PGL and GIST [17]; and 3P association syndrome (3PAs) for pheochromocytoma, PGL, and PA [18].

1. Materials and Methods

Following negative results from comprehensive PPGL gene testing in standard commercial NGS facilities, we investigated 2 families with various neoplasms, including PGL, GIST, RCC, and PA. We hypothesized that their tumor predilection may be due to a mutation in a novel *PPGL* gene or in a location in a known *PPGL* gene leading to altered gene transcription or expression that is not captured by standard genetic testing.

All clinical data were collated and updated prior to manuscript preparation in July 2019. All genetic investigations were performed in a clinical setting by nationally accredited laboratory processes. Prospective written consent to testing was obtained from all living patients, and from next of kin in the case of deceased relatives, prior to the genetic investigations. Subsequently, written consent to publication was obtained from all living patients and from next of kin in the case of deceased relatives. The publication was ethically approved by the Royal Adelaide Hospital Human Research Ethics Committee in accordance with the National Health and Medical Research Council guidelines.

A. Case Descriptions

Pedigrees of the 2 Italian-Australian families are shown in Fig. 1 and clinical features are listed in Table 1. Genetic and IHC test results are summarized in Supplemental Table 1 [19].
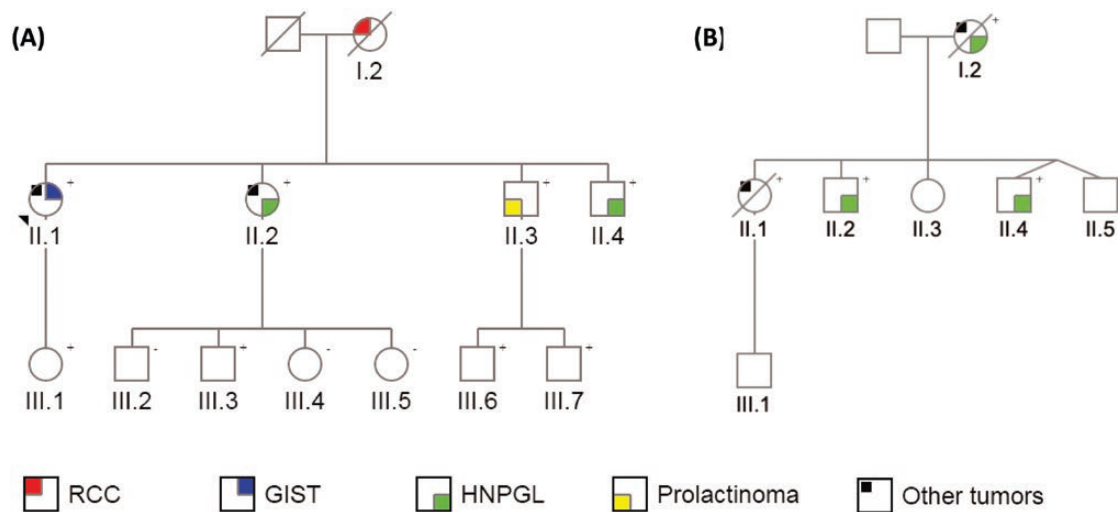
A-1. Family 1

The index family was of Italian ethnicity and consisted of 4 siblings with SDH-related tumors, with their mother having died from RCC. Preliminary genetic testing in the proband, II.2, was negative for *SDHB*, *SDHC*, *SDHD*, *SDHAF2*, *VHL*, *RET*, and *TMEM127* mutations by direct gene sequencing, and for *SDHB*, *SDHC*, *SDHD*, and *VHL* copy number variants (CNVs) by multiplex ligation-dependent probe amplification (MLPA).

I.2, a lifelong nonsmoker, was diagnosed with RCC at age 60 years and underwent left nephrectomy, demonstrating an 8.5-cm RCC with focal sarcomatoid appearance, microscopic invasion of perinephric fat, and metastasis to peripelvic fat. SDHB tumor IHC was historically reported

as positive, although the tissue slides are no longer available for review.

II.1 first presented with a multifocal mesenteric desmoid tumor at age 50. She underwent right hemicolectomy at diagnosis, followed by small bowel and mesenteric resection and medical therapy with ibuprofen, tamoxifen, celecoxib, and letrozole at age 54, and small bowel and sigmoid resection at age 55 for recurrent disease. Also at age 50, she was diagnosed with a well-differentiated hepatocellular carcinoma (HCC) for which she underwent resection at age 51 and radiofrequency ablation of a presumed second lesion at age 52. There was no evidence of HCC metastasis on computed tomography imaging or whole-body bone scan. At age 51, she underwent resection of 2 gastric GISTs, measuring 6 mm at the lesser gastric curve and 20 mm at the body of the stomach. At age 53, she was found to have an 11-mm nonfunctioning adrenocortical adenoma that is being monitored, and a solitary fibrous tumor of the lung that was resected. She was most recently diagnosed with a 4.2-cm left frontal meningioma at age 59 and is awaiting further management. SDHB IHC was performed on the desmoid tumor, HCC, and GIST, with all samples showing positive staining. The 2 GIST specimens shared a similar appearance, with predominant spindle cell morphology and positive IHC for c-Kit/CD117 and Discovered on GIST-1 (DOG1), all of which suggested a receptor tyrosine kinase–mediated tumor.

II.2 presented with a nonsecretory left cerebellopontine PGL at age 41 and underwent partial resection following embolization. SDH tumor IHC was negative for SDHB and positive for SDHA. She recently completed radiotherapy at age 57 for the PGL remnant, which reached a diameter of 4.2 cm and was encasing the left internal carotid artery

Figure 1. Pedigrees of A, family 1 and B, family 2, highlighting succinate dehydrogenase (SDH)-related and other tumors in affected family members. Genetic status regarding the intronic *SDHC* variant c.20 + 74A >G is indicated in the top right-hand corner for all tested individuals. [+], variant present; [–], variant absent.

Table 1. Tumor phenotype in affected relatives of family 1 and family 2

Family	Individual (current age)	*SDHC* mutation status	Tumors (age at initial diagnosis, y)	SDHB tumor IHC	Succinate:fumarate ratio
1	I.2 (died 61)	N/T	RCC (60)	Positive	N/T
	II.1 (59)	+	Desmoid tumor (50)	Positive	10.600, 16.037, 11.681[a]
			HCC (50)	Positive	29.458
			Gastric GIST (51)	Positive	41.765, 6.815[b]
			Solitary fibrous tumor of lung (53)	N/T	13.895
			Adrenocortical adenoma (53)	N/T	N/T
			Meningioma (59)	N/T	N/T
	II.2 (57)	+	HNPGL (41)	Negative	89.490
			Ovarian serous cystadenoma and cellular fibroma (53)	N/T	11.644
			Meningioma (54)	N/T	N/T
	II.3 (54)	+	Prolactinoma (41)	N/T	N/T
	II.4 (52)	+	HNPGL (34)	Negative	27.725
2	I.2 (died 61)	+	HNPGL (44)	Negative	N/T
			Breast cancer (44)	N/T	N/T
			Cholangiocarcinoma (61)	N/T	N/T
	II.1 (died 38)	+	Diffuse gastric carcinoma (38)	Positive	N/T
	II.2 (38)	+	Suspected HNPGL (37)	N/T	N/T
	II.4 (34)	+	HNPGL (20)	Negative	N/T

Abbreviations: +, mutation present; GIST, gastrointestinal stromal tumor; HCC, hepatocellular carcinoma; HNPGL, head and neck paraganglioma; IHC, immunohistochemistry; N/T, not tested; RCC, renal cell carcinoma.
[a]Multiple ratios determined from serial resections of recurrent desmoid tumor.
[b]Multiple ratios determined from multifocal gastric GIST resected simultaneously.

and impinging on the brainstem. She was also diagnosed with an ovarian serous cystadenoma and ovarian cellular fibroma, both resected at age 53, and a parafalcine meningioma at age 54 that is under imaging surveillance.

II.3 was diagnosed with a 3.4-cm macroprolactinoma at age 41. He achieved a complete hormonal and tumor response with cabergoline.

II.4 was diagnosed with a nonsecretory, multifocal, skull base PGL at age 34 and underwent partial resection following embolization. The PGL remnant is stable on serial monitoring. SDH tumor IHC was negative for SDHB and positive for SDHA.

Because of the family history of PGL, all members of the second and third generations of family 1 apart from III.5 have been screened for PPGL via magnetic resonance imaging every 2 to 3 years and annual plasma metanephrines with no evidence of PPGL to date in any relatives other than II.2 and II.4.

A-2. Family 2

The second family was noteworthy for SDH-related and other neoplasia in 2 siblings and their mother. Preliminary genetic testing in the proband with PGL, II.4, was negative for *SDHB*, *SDHC*, *SDHD*, *SDHAF2*, *VHL*, *RET*, and *TMEM127* mutations by direct gene sequencing, and for *SDHB*, *SDHC*, *SDHD*, and *VHL* CNVs by MLPA. All preliminary genetic tests in II.1, performed because of her history of gastric cancer, were negative, including *CDH1*, *CTNNA1*, *MLH1*, *MSH2*, *MSH6*, *EPCAM*, *BRCA1*, and *BRCA2* by NGS; *BRCA1*, *BRCA2*, and *PMS2* by direct gene sequencing; and *CDH1*, *MLH1*, *MSH2*, *MSH6*, *EPCAM*, and *PMS2* by MLPA. In view of the negative genetic test results and shared Italian ethnicity, family 2 was selected for investigation for the mutation identified in family 1 during the course of this study.

I.2 was diagnosed with a right jugular PGL at age 44 and underwent resection following embolization. Histopathology confirmed PGL with lymph node metastases. SDHB IHC was negative (SDHA IHC not performed). She was concurrently diagnosed with breast cancer, treated with mastectomy, axillary clearance, and adjuvant chemoradiotherapy. She remained in remission of her PGL and breast cancer at age 61, when she died of newly diagnosed metastatic cholangiocarcinoma.

II.1 presented with acute kidney injury and venous thromboembolism 2 months postpartum at age 38. She died from a presumed systemic inflammatory illness with multiple osteolytic lesions 3 weeks later. Postmortem examination revealed metastatic diffuse gastric carcinoma. Tumor IHC was positive for SDHB and SDHA.

II.4 underwent resection for a right jugulotympanic PGL at age 20. SDH tumor IHC was negative for SDHB and positive for SDHA.

The surviving second-generation members of family 2 recently underwent PPGL screening, revealing a likely head and neck PGL (HNPGL) recurrence in II.4 and a new diagnosis of likely HNPGL in II.2. PPGL screening was negative in II.3 and II.5.

B. DNA Extraction

Fresh blood samples were obtained from II.1 to 4 of family 1 and II.4 of family 2 for extraction of germline DNA from peripheral blood leukocytes. Among the deceased individuals, no DNA was available from I.2 of family 1, stored DNA was obtained from II.1 of family 2, and only tumor DNA was available from I.2 of family 2. Tumor DNA extraction was performed using formalin-fixed, paraffin-embedded (FFPE) tissue specimens of the 6-mm GIST in II.1 and the PGL in II.4 in family 1, and the PGL and breast cancer in I.2 in family 2. Other tumor specimens were not available for sequencing. Germline and tumor DNA were extracted using commercially available kits (Qiagen) according to manufacturer protocols.

C. Whole-Exome Sequencing

Whole-exome sequencing (WES) was performed in family 1 using the available germline and tumor DNA samples, the Roche NimbleGen SeqCap EZ MedExome Target Enrichment Kit, and the Illumina NextSeq 500 sequencing platform. The average of mean depth of coverage among all samples was 97×, and 94% of target bases were covered at 20× or greater. Bioinformatic analysis was performed at ACRF in Adelaide, Australia, using Genome Analysis Toolkit (GATK) HaplotypeCaller to detect small variants (typically < 50 base pairs, bp) and in-house scripts and Sequenza to analyze CNVs. Raw WES data were filtered for variants that were rare (< 1% population prevalence), possibly damaging (by snpEFF impact, splicing/binding predictions, or Genomic Evolutionary Rate Profiling [GERP] or Combined Annotation Dependent Depletion scores), and of high quality (by GATK internal filters). Germline variants were considered further if they were heterozygous in the germline DNA of all 4 siblings in family 1 with a GATK genotype quality score greater than 50 and depth of coverage greater than 30×. Variants in low-complexity regions or duplicated segments were discarded. Candidate genes were prioritized based on existing literature. In silico splice site assessment was performed using Alamut Visual, incorporating SpliceSiteFinder-like, MaxEntScan, NNSPLICE, and GeneSplicer prediction models.

The Roche NimbleGen SeqCap EZ MedExome Target Enrichment Kit and the Illumina NextSeq 500 sequencing platform were also employed in the preliminary testing of gastric cancer predisposition genes in II.1 of Family 2.

D. Sanger Sequencing

The leading germline variant of interest in family 1 was assessed using germline DNA from II.1 to 4 of family 1 and II.1 and II.4 of family 2, and tumor DNA from I.2 from family 2. Bidirectional genomic DNA sequencing was performed using primers designed via Primer3Plus and raw data were visualized using MutationSurveyor version 2.51 (SoftGenetics LLC).

Sanger sequencing for the leading germline variant of interest was later performed to facilitate predictive cascade testing in other relatives of family 1 and family 2.

E. Haplotype Analysis

Haplotype analysis was performed by considering rare variants (SNPs > 20× coverage, ExAC and UK10K allele frequencies < 0.01) in the WES data of II.2 of family 1 and II.1 of family 2 and mapping those loci that overlapped between the 2 individuals. For any rare variant identified in either individual, an unrelated individual would overlap at less than 1% of loci with random distribution throughout the genome. Conversely, relatedness due to identity by descent would be identified by a chain of shared rare variants that are nonrandomly distributed throughout the genome.

F. Transcriptome Analysis

Whole blood was obtained from II.2 of family 1 for transcriptome analysis to further investigate the leading germline variant of interest in family 1. RNA sequencing (RNA-Seq) was performed via the Illumina TruSeq LT platform using 150 bp reads and poly(A) selected RNA to deplete ribosomal RNA. Messenger RNA–enriched RNA-Seq libraries from the patient were sequenced on the Illumina NextSeq 500 platform using the stranded, paired-end protocol with a read length of 150 bp. Raw reads were adapter-trimmed and filtered for short sequences using Cutadapt v1.16, setting the minimum length option to 18, overlap 5 and error rate 0.2. The resulting FASTQ file containing 26.6 million read pairs was analyzed and quality-checked using the FastQC program (http://www.bioinformatics.babraham.ac.uk/projects/fastqc). Reads were mapped against the human reference genome (hg19) using the STAR spliced alignment algorithm (v2.5.3a with default parameters and –chimSegmentMin 20, –quantMode GeneCounts),

returning an average unique alignment rate of 88.0%. Read alignments, including spliced reads, were visualized, interrogated, and graphically represented using the Integrative Genomics Viewer v2.3.80.

G. Krebs Cycle Metabolomic Studies

Available FFPE tumor specimens from the index family were tested in duplicate by mass spectrometry to measure succinate and fumarate levels and calculate succinate:fumarate ratios to aid the identification of SDH-deficient tumors as previously described [9]. Briefly, analysis of extracts was performed on a Prominence high-performance liquid chromatography system (Shimadzu) coupled to an API QTRAP 5500 mass spectrometer (SCIEX). Separation of target analytes from isobaric interferences was achieved using an Ascentis Express 100 Å~3.0 mm 2.7 µmRP Amide (Sigma-Aldrich) analytical column held at 40°C and isocratic elution using aqueous 0.4% formic acid with a flow rate of 0.5 mL/min. We routinely included certified reference materials for succinate and fumarate (Sigma-Aldrich). Multiple reaction monitoring with negative electrospray ionization was used for quantification. Each sample was run in duplicate, with an intra-assay coefficient of variation for succinate of 22% and for fumarate of 21%. Positive and negative controls were included in each run. We had previously determined a threshold for the succinate:fumarate ratio of 23.48 in SDH-deficient GIST FFPE specimens [9]. Recognizing that succinate:fumarate ratios are typically lower in HNPGL compared to sympathetic PGLs [20, 21], and in FFPE compared to fresh-frozen specimens [2, 21], we cautiously adopted a succinate:fumarate ratio of 65.00 that identifies most SDH-deficient PGLs [9].

H. SDHC *Promoter Methylation Analysis*

Methylation status of the *SDHC* promoter region was determined in both GIST specimens from family 1 II.1. A Pyromark CpG assay was performed as previously described [22]. A total of 1500 ng of sample DNA was used for bisulfite conversion treatment in individual polymerase chain reaction (PCR) tubes, with 3 bisulfite conversion periods (60°C × 25 minutes, 60°C × 85 minutes, and 60°C × 175 minutes), separated by 3 DNA denaturation periods and followed by column purification as per the manufacturer's instructions (Qiagen, EpiTect Bisulfite Kit, catalog No. 59104). Bisulfite-converted DNA was amplified using the PyroMark PCR Kit (catalog No. 978703) using primers targeting 4 CpG sites of the *SDHC* promoter (Chr1: 161 313 986; Chr1: 161 313 998; Chr1: 161 314 011, and Chr1: 161 314 022). Qiagen Epitec Control DNA, methylated (catalog No. 59655) and unmethylated (catalog No. 59665), were included as the assay quality controls. Following PCR, the

amplicons were immobilized and single-strand templates produced via Streptavidin Sepharose High Performance beads (GE Healthcare, 17-5113-01), followed by annealing of the sequencing primer to the template. The samples were then analyzed on the PyroMark Q24 system, using PyroMark Gold Q24 Reagents Kit (catalog No. 970802) for quantitative measurement of methylation in 4 CpG sites of the *SDHC* promoter. Sequences surrounding the defined positions served as normalization and reference peaks for quantification and quality assessment of the analysis. Pyrograms were analyzed using Pyromark Q24 software (Qiagen), version 2.0.6, to calculate percentage methylation at each CpG, and mean methylation across all CpGs for each sample was calculated.

2. Results

A. Germline Genetic Analysis in Family 1

After filtration of raw data, WES of germline DNA revealed 19 581 rare variants with at least some evidence of pathogenicity, including 130 high-quality heterozygous variants in all 4 siblings of family 1. One variant was found in an intronic region of the known candidate gene, *SDHC* (GRCh37/hg19, Chr1:g.161284289A > G; NM_003001; c.20 + 74A>G; Fig. 2A), at greater than 20× coverage (21 wild-type [WT] reads, 32 mutant allele reads in II.1; 93,80 in II.2; 25,24 in II.3; and 35,30 in II.4). Sanger sequencing confirmed the variant in all 4 siblings (Fig. 2D). This *SDHC* intronic variant is situated in a conserved region (GERP 2.38) of intron 1 and has not been previously reported. It is absent in public genomic datasets, including: 1KGP; UK10K; ExAC; and gnomAD, containing 31 378 control alleles in the vicinity of this variant, including 106 alleles from patients of Southern European ethnicity. All 4 component splicing models of Alamut Visual predicted introduction of an alternate 5' (donor) splice site at the location of the variant.

Subsequent RNA-Seq of whole blood from II.2 of family 1 showed aberrant splicing of *SDHC* with messenger RNA reads extending into intron 1 (Fig. 2B), due to conversion of a nonsplicing region (TG|AT) into a canonical splice site (TG|GT) because of the familial *SDHC* variant. There was evidence of preferential expression of the alternatively spliced transcript (n = 114) compared to the normal transcript (n = 46) (Fig. 2C). The alternatively spliced transcript is absent in publicly accessible databases (UCSC Genome Browser, Ensembl, GTEx, NCBI) as well as in-house RNA-Seq results from more than 700 samples.

The retained segment size is 75 bp due to the upstream inclusion of a common 2-bp *SDHC* insertion listed as benign by ClinVar (*SDHC*, NM_003001.3, c.20 + 11_20 + 12dupTG). Thus, frameshift does not occur. However, the retained intronic segment produces a premature stop codon immediately after exon 1. The final SDHC

protein product is significantly shortened (Fig. 2E) and predicted to result in nonsense-mediated decay.

Overall, the familial *SDHC* variant fulfilled the American College of Medical Genetics and Genomics criteria for a pathogenic (class 5) variant (PVS1: null variant, PS3: functional evidence, PM2: absent from controls, PP1: cosegregation) [23].

Given the history of additional tumors in II.1 and II.2, germline data from these individuals was independently interrogated for variants in genes predisposing to GIST (*KIT*, *PDGFRA*), meningioma (*NF2*, *SMARB1*, *SMARCE1*, *SUFU*, *LZTR1*), and desmoid tumors (*APC*). Applying our basic filters, we found no germline variants in these genes.

B. Tumor Genetic Analysis in Family 1

WES and copy number analysis of the PGL from II.4 of Family 1 revealed 0.4-0.5X ploidy loss of chromosome (Chr) 1 (Fig. 3). This may represent either loss of one copy of Chr

1 in 40% to 50% of tumor cells or loss of both copies of Chr 1 in 20% to 25% of tumor cells. Mutant allele frequency would be expected to be unchanged if both chromosomes were lost in a subset of cells or if there were unbiased loss of Chr 1 between different cells. By contrast, the *SDHC* intronic variant load on WES rose from 47% in II.4's germline DNA to 60% in II.4's tumor DNA. It was thus deduced that 40% of cells lost the *SDHC* WT allele (producing a 3:5 WT:mutant ratio in tumor DNA vs a 1:1 ratio in heterozygous germline DNA). This chromosomal loss was considered to be the second hit in the tumor-suppressor gene 2-hit model, thus supporting the germline *SDHC* intronic variant as the causative mutation. Whole chromosome loss of Chr 11 was also detected, as is commonly observed in PGL specimens [24].

WES of the 6-mm GIST from II.1 of family 1 demonstrated a previously described [25] gain-of-function *KIT* mutation (GRCh37/hg19, Chr2:g.55593610T > G; ENST00000288135; p.Val559Gly/c.1676T > G). Other
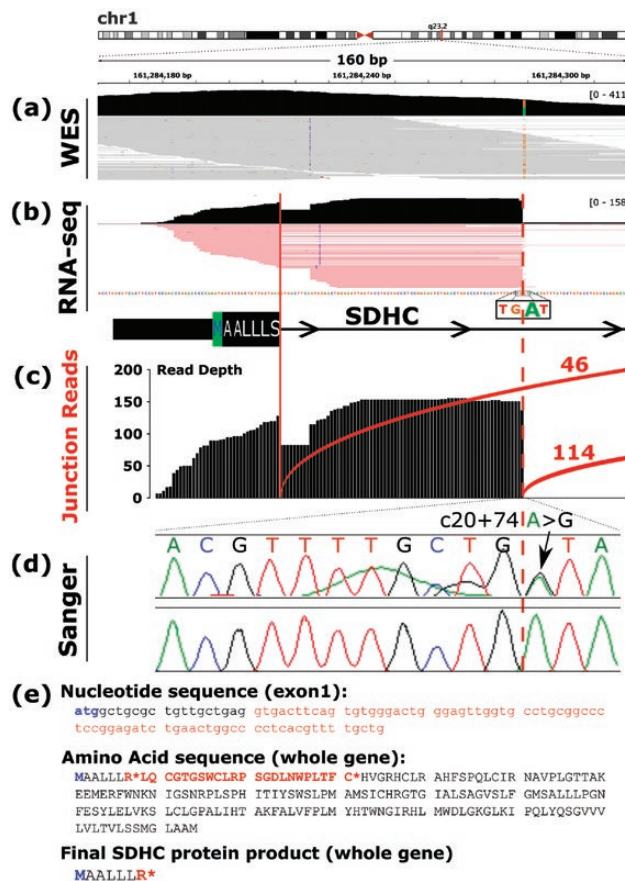
Figure 2. DNA and RNA representations of the intronic *SDHC* variant c.20 + 74A > G in II.2 of family 1. A, Whole-exome sequencing result of germline DNA as depicted in Integrative Genomics Viewer. The heterozygous substitution of guanine (brown) for adenosine (green) is shown at genomic DNA position 161 284 289. B, RNA sequencing (RNA-Seq) result as depicted in Integrative Genomics Viewer showing alternative splicing of exon 1. The canonical splice site is indicated by the solid red line and the novel splice site by the dotted red line, coinciding with the A > G substitution. C, Junction counts of individual messenger RNA reads showing preferential expression of the aberrantly spliced transcript (n = 114) vs normal transcript (n = 46). D, Electrophoretogram confirming the germline DNA variant. E, Nucleotide, amino acid, and final protein product sequences produced by the 75-bp inclusion observed on RNA-Seq. The start codon is indicated in blue. The intronic inclusion in exon 1 created by the *SDHC* c.20 + 74A > G variant is indicated in red, and premature stop codons are indicated by the red asterisks.

than the germline c.20 + 74A > G variant, no point mutations or copy number variants involving *SDHC* were found in this specimen. Each of the noncontiguous GIST specimens from II.1 of family 1 showed low *SDHC* promoter methylation: range 7% to 24%, average 15.3% in the 6-mm GIST; range 9% to 22%, average 14.8% in the 20-mm GIST. Further data are presented in Supplemental Table 2 and Supplemental Fig. 1 [19]. The methylation rate in these tumors fell in the bottom 10% of internal FFPE GIST control specimens (n = 15) [9], excluding *SDHC* promoter hypermethylation in the pathogenesis of this patient's GISTs.

C. Genetic Linkage Between Family 1 and Family 2

Sanger sequencing in family 2 using germline DNA from II.1 and II.4 and tumor DNA from the PGL and breast cancer of I.2 revealed the same *SDHC* intronic variant in these 3 family members with neoplasia. Because hotspot mutations have not been described in *SDHC* and because of the shared Italian ancestry of families 1 and 2, haplotype analysis was performed to investigate cryptic relatedness. This demonstrated multiple regions of identity by descent, including the *SDHC* gene, consistent with a shared common ancestor (Fig. 4). Expanded family history-taking revealed that the 2 families originated from the same small region in Italy.

D. Metabolomic Profiles

Succinate:fumarate ratios derived from the available tumors of family 1 are shown in Table 1. A high succinate:fumarate ratio consistent with SDH deficiency was documented in the PGL from II.2, in concordance with the negative SDHB IHC result for this tumor. The 6-mm GIST specimen from II.1 also exhibited a succinate:fumarate ratio consistent with SDH deficiency despite positive SDHB IHC, the WES finding of a known *KIT* mutation in this particular GIST specimen, and an SDH-sufficient ratio in the 20-mm GIST specimen from the same patient. The PGL from II.4 demonstrated an equivocal succinate:fumarate ratio, whereas SDHB IHC classified this tumor as SDH deficient. There is a lack of normative data with which to compare the ratios of the other tumor types; the ratios in Table 1 are provided for reference only. Overall, there was inconsistency between the metabolomic profiles and IHC results for the various neoplasms and the latter was prioritized as the gold standard by which to determine SDH deficiency.

E. Cascade Testing

The c.20 + 74 A > G *SDHC* variant was subsequently detected in III.1, III.3, III.6, and III.7 of family 1, and in II.2 of family 2. Apart from II.2 of family 2, who was recently diagnosed with a likely HNPGL, all of these mutation carriers appear to be unaffected to date.

The variant was absent in III.2, III.4, and III.5 of family 1, and in II.5 of family 2.

Cascade testing has not yet been performed in II.3 and III.1 of family 2.

3. Discussion

The *SDHC* intronic variant reported here is the deepest intronic variant to be reported among the *SDHx* genes, highlighting aberrant splicing as an important consideration in patients with unexplained familial PPGL syndromes and other SDH-deficient tumors. This was
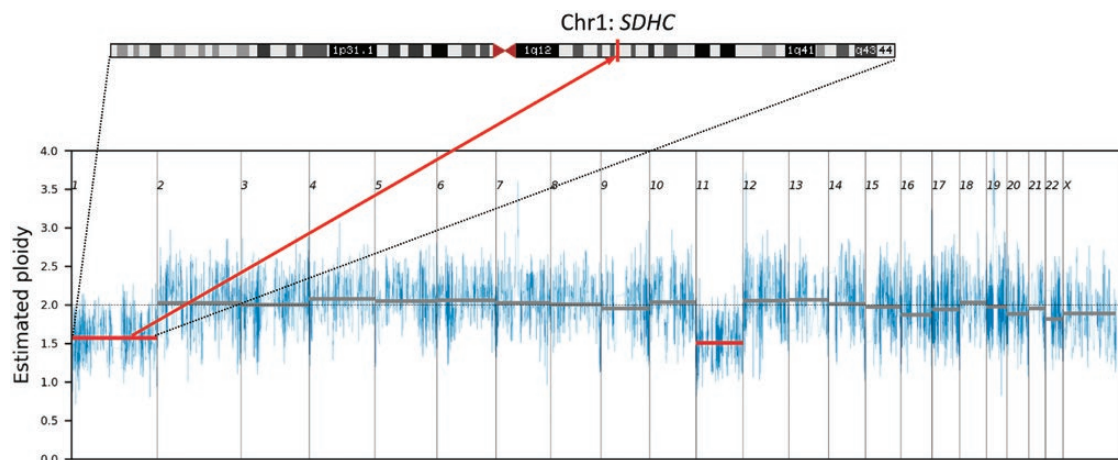
Figure 3. Chromosome 1 and 11 loss as demonstrated by tumor DNA whole-exome sequencing in the paraganglioma of II.4 from family 1. The position of the *SDHC* gene on chromosome 1 is indicated.

Figure 4. Haplotype analysis using exome data from each of the 22 autosomes showing regions unique to family 1 in red, regions unique to family 2 in green, and regions shared between the 2 families in blue. The multiple shared regions throughout the genome indicate identity by descent, and therefore a shared common ancestor between family 1 and family 2. The inset shows the shared region on chromosome 1 that includes *SDHC*.

identified in 2 families with historical links to the same small region in Italy who were shown to be distantly related by haplotyping. Contrary to the fortuitous finding in this WES study, intronic variants beyond the first 10 bp of exon-intron junctions will usually be missed by WES as well as the NGS gene panels typically used in the clinical testing of PPGL patients. Whole-genome sequencing, though more costly, may be required in PPGL cases with negative routine genetic testing despite a characteristic phenotype. The extent to which this is necessary will depend on the frequency of intronic *SDHx* mutations in unexplained SDH-deficient tumor syndromes, noting that 18% to 19% of patients with SDH-deficient tumors by IHC lack identifiable *SDHx* mutations by current testing methodologies [26, 27].

SDH-related tumors have been described in the setting of a range of germline *SDHx* variant types, including start codon, missense, nonsense, and frameshift variants, and whole exon and gene deletions [1, 28]. Epigenetic variation has also been described with *SDHC* promoter hypermethylation now known to account for Carney triad [29] and the half of SDH-deficient GISTs that were previously considered unexplained because of a lack of germline *SDHx* mutations [2, 3]. Splice site mutations are another known mechanism of tumorigenesis, with germline *SDHC* splicing variants accounting for 15% of PGLs and 30% of GISTs [1]. However, such splicing variants are typically only 1 to 2 bp away from the intron-exon boundary. Of 557 publicly available *SDHx* variants reported in the Leiden Open Variant Database (http://www.lovd.nl/3.0/home) as anything but benign or likely benign, only 38 variants are intronic and suspected or proven to cause aberrant splicing according to the submitted classification. The deepest of such variants are only ±7 bp away from the exon-intron boundary. While the term *deep intronic variant* is reserved for variants more than 100 bp away from exon-intron boundaries [30], the c.20 + 74A > G *SDHC* variant is important to recognize because it falls outside the usual 10- to 20-bp region that is typically assessed in clinical genetic testing, explaining why the variant was undetected in the preceding sequential genetic testing that spanned 12 years in family 1.

The *SDHC*-related familial PGL syndrome (also referred to as hereditary PGL syndrome type 3; PGL3) is widely considered to be a less severe disorder than the more common

familial syndromes associated with *SDHD* (PGL1) and *SDHB* (PGL4) mutations [3, 31]. PGL3 typically manifests as unifocal nonsecretory HNPGL with low malignant potential, reduced risk of RCC and PA, and overall low penetrance [3]. Consistent with this classical phenotype, our families developed nonsecretory HNPGLs with metastasis in only one case. All PGLs stained negative for SDHB and positive for SDHA, as expected. Furthermore, the one PGL available for WES exhibited Chr 1 loss consistent with loss of the WT *SDHC* allele.

Unusually for the *SDHC* gene in particular, family 1 also exhibited the other 3 tumor types that have been previously linked to SDH deficiency. However, none of these tumors was proven to be SDH deficient in this family. The RCC was deemed sufficient by SDHB IHC performed soon after surgery around the advent of SDH IHC, but contemporary IHC studies, metabolomic profiling, and WES were not possible in this specimen, which was later destroyed, or in the macroprolactinoma that was successfully treated with a dopamine agonist. The GIST stained positive for KIT, showed normal SDHB IHC, and had predominant spindle cell morphology, all consistent with the somatic gain-of-function *KIT* mutation found on WES. Metabolomic analysis conversely showed one GIST specimen to have a significantly increased succinate:fumarate ratio suggestive of SDH deficiency, although the limited evidence base of metabolomic profiling compared to SDHB IHC is recognized. Furthermore, we did not identify any *SDHC* somatic second hits on WES of the GIST and *SDHC* promoter hypermethylation studies were negative.

We observed other tumors that have been previously reported in patients with *SDHx* abnormalities—adrenocortical adenoma [16, 31, 32], meningioma [33], breast cancer [1, 33] and diffuse gastric cancer [34, 35]—as well as tumors that have not been previously linked with *SDHx* mutations—HCC, desmoid tumor, solitary fibrous tumor of the lung, ovarian serous cystadenoma, ovarian cellular fibroma and cholangiocarcinoma. Whether any of these tumors relate to the germline *SDHC* mutation remains to be elucidated because these tumors were either shown to be SDH sufficient by IHC or were unavailable for investigation. Succinate:fumarate ratios were calculated in available tumors, but the significance of these results is limited by the lack of comparative tumor-specific data.

Although most of the tumors in these families are individually rare and the combination of tumors would be exceedingly rare, we cannot exclude the incidental co-occurrence of sporadic tumors. Another possibility is multiple inherited neoplasia allele syndrome (known as MINAS) [36]; however, WES did not demonstrate suspicious germline variants in other relevant tumor predisposition genes. The apparently high burden of tumors in *SDHx* mutation carriers may also relate to close surveillance, especially in the absence of definitive evidence of SDH deficiency in the tumors.

The cryptic relatedness suspected in these families because of their shared ethnicity was confirmed by a contemporary form of haplotype analysis in which identity by descent was determined by comparing rare variants deduced from NGS and ExAC reference data. This methodology may be used to evaluate other suspected *SDHx* founder mutations. A partial *SDHC* gene deletion in apparently unrelated patients of Yemenite ethnicity has been suggested but unproven to be due to a founder mutation [31]. Previous genealogy work using demographic data traced a large cohort of French-Canadian patients with *SDHC*-related PGLs due to a truncating founder mutation [37]. Confirming cryptic relatedness is not only of biological interest, but also clinically significant as it guides cascade testing.

In conclusion, we report a novel *SDHC* pathogenic variant, c.20 + 74A > G, which represents the deepest intronic mutation in an *SDHx* gene. Although we showed the PGLs in these families to be SDH deficient, conclusive results were not reached in the other tumors that either showed positive SDHB IHC or were unable to be studied because of a lack of tumor specimens. Further research is required to assess the causative role of this *SDHC* mutation in the wide tumor spectrum described here. For now, *SDHx* intronic mutations should be considered in patients with SDH-related tumor types, especially in the approximately 20% of SDH-deficient tumors with no identifiable mutation on routine genetic testing [26, 27]. Large validation studies are required to determine the cost-benefit analysis of targeted testing for intronic mutations—for example, through RNA-Seq—in patients with PPGL and other seemingly inherited disorders [38].

Additional Information

Correspondence: Sunita M.C. De Sousa, MBBS (Hons), MSc, PhD, FRACP, Endocrine and Metabolic Unit, Area 8G-480 Royal Adelaide Hospital, Port Rd, Adelaide, South Australia 5000, Australia. E-mail: Sunita.DeSousa@sa.gov.au.

Disclosure Statement: The authors have nothing to disclose.

Data Availability: Restrictions apply to the availability of data generated and analyzed during this study to preserve patient confidentiality. The corresponding author will on request detail the restrictions and any conditions under which access to some data may be provided.

References

1. Evenepoel L, Papathomas TG, Krol N, et al. Toward an improved definition of the genetic and tumor spectrum associated with SDH germ-line mutations. *Genet Med.* 2015;**17**(8):610-620.

2. Gill AJ. Succinate dehydrogenase (SDH)-deficient neoplasia. *Histopathology.* 2018;**72**(1):106-116.

3. Benn DE, Robinson BG, Clifton-Bligh RJ. 15 Years of paraganglioma: clinical manifestations of paraganglioma syndromes types 1-5. *Endocr Relat Cancer.* 2015;**22**(4):T91-T103.

4. Eijkelenkamp K, Osinga TE, Links TP, van der Horst-Schrivers ANA. Clinical implications of the oncometabolite succinate in *SDHx*-mutation carriers. *Clin Genet.* 2020;**97**(1):39-53.

5. Toledo RA, Burnichon N, Cascon A, et al. Consensus statement on next-generation-sequencing-based diagnostic testing of hereditary phaeochromocytomas and paragangliomas. *Nat Rev Endocrinol.* 2017;**13**(4):233-247.

6. van Nederveen FH, Gaal J, Favier J, et al. An immunohistochemical procedure to detect patients with paraganglioma and phaeochromocytoma with germline *SDHB*, *SDHC*, or *SDHD* gene mutations: a retrospective and prospective analysis. *Lancet Oncol.* 2009;**10**(8):764-771.

7. Gill AJ, Benn DE, Chou A, et al. Immunohistochemistry for SDHB triages genetic testing of *SDHB*, *SDHC*, and *SDHD* in paraganglioma-pheochromocytoma syndromes. *Hum Pathol.* 2010;**41**(6):805-814.

8. Gill AJ, Chou A, Vilain R, et al. Immunohistochemistry for *SDHB* divides gastrointestinal stromal tumors (GISTs) into 2 distinct types. *Am J Surg Pathol.* 2010;**34**(5):636-644.

9. Kim E, Wright MJ, Sioson L, et al. Utility of the succinate:fumarate ratio for assessing SDH dysfunction in different tumor types. *Mol Genet Metab Rep.* 2017;**10**:45-49.

10. Lenders JW, Duh QY, Eisenhofer G, et al; Endocrine Society. Pheochromocytoma and paraganglioma: an Endocrine Society clinical practice guideline. *J Clin Endocrinol Metab.* 2014;**99**(6):1915-1942.

11. Neumann HP, Bausch B, McWhinney SR, et al; Freiburg-Warsaw-Columbus Pheochromocytoma Study Group. Germline mutations in nonsyndromic pheochromocytoma. *N Engl J Med.* 2002;**346**(19):1459-1466.

12. Sbardella E, Cranston T, Isidori AM, et al. Routine genetic screening with a multi-gene panel in patients with pheochromocytomas. *Endocrine.* 2018;**59**(1):175-182.

13. Brito JP, Asi N, Bancos I, et al. Testing for germline mutations in sporadic pheochromocytoma/paraganglioma: a systematic review. *Clin Endocrinol (Oxf).* 2015;**82**(3):338-345.

14. Currás-Freixes M, Piñeiro-Yañez E, Montero-Conde C, et al. PheoSeq: a targeted next-generation sequencing assay for pheochromocytoma and paraganglioma diagnostics. *J Mol Diagn.* 2017;**19**(4):575-588.

15. Buffet A, Ben Aim L, Leboulleux S, et al; French Group of Endocrine Tumors (GTE) and COMETE Network. Positive impact of genetic test on the management and outcome of patients with paraganglioma and/or pheochromocytoma. *J Clin Endocrinol Metab.* 2019;**104**(4):1109-1118.

16. Carney JA. Gastric stromal sarcoma, pulmonary chondroma, and extra-adrenal paraganglioma (Carney triad): natural history, adrenocortical component, and possible familial occurrence. *Mayo Clin Proc.* 1999;**74**(6):543-552.

17. Carney JA, Stratakis CA. Familial paraganglioma and gastric stromal sarcoma: a new syndrome distinct from the Carney triad. *Am J Med Genet.* 2002;**108**(2):132-139.

18. Xekouki P, Szarek E, Bullova P, et al. Pituitary adenoma with paraganglioma/pheochromocytoma (3PAs) and succinate dehydrogenase defects in humans and mice. *J Clin Endocrinol Metab.* 2015;**100**(5):E710-E719.

19. De Sousa S, Toubia J, Hardy TSE, et al. Aberrant splicing of *SDHC* in families with unexplained succinate dehydrogenase-deficient paragangliomas - supplementary material. *Figshare.* Deposited 4 September 2020. doi:10.6084/m9.figshare.12917279.v1

20. Richter S, Gieldon L, Pang Y, et al. Metabolome-guided genomics to identify pathogenic variants in isocitrate dehydrogenase, fumarate hydratase, and succinate dehydrogenase genes in pheochromocytoma and paraganglioma. *Genet Med.* 2019;**21**(3):705-717.

21. Richter S, Peitzsch M, Rapizzi E, et al. Krebs cycle metabolite profiling for identification and stratification of pheochromocytomas/paragangliomas due to succinate dehydrogenase deficiency. *J Clin Endocrinol Metab.* 2014;**99**(10):3903-3911.

22. Flanagan S, Lee M, Li CC, Suter CM, Buckland ME. Promoter methylation analysis of *IDH* genes in human gliomas. *Front Oncol.* 2012;**2**:193.

23. Richards S, Aziz N, Bale S, et al; ACMG Laboratory Quality Assurance Committee. Standards and guidelines for the interpretation of sequence variants: a joint consensus recommendation of the American College of Medical Genetics and Genomics and the Association for Molecular Pathology. *Genet Med.* 2015;**17**(5):405-424.

24. Dannenberg H, de Krijger RR, Zhao J, et al. Differential loss of chromosome 11q in familial and sporadic parasympathetic paragangliomas detected by comparative genomic hybridization. *Am J Pathol.* 2001;**158**(6):1937-1942.

25. Joensuu H, Rutkowski P, Nishida T, et al. KIT and PDGFRA mutations and the risk of GI stromal tumor recurrence. *J Clin Oncol.* 2015;**33**(6):634-642.

26. Castelblanco E, Santacana M, Valls J, et al. Usefulness of negative and weak-diffuse pattern of SDHB immunostaining in assessment of SDH mutations in paragangliomas and pheochromocytomas. *Endocr Pathol.* 2013;**24**(4):199-205.

27. Papathomas TG, Oudijk L, Persu A, et al. SDHB/SDHA immunohistochemistry in pheochromocytomas and paragangliomas: a multicenter interobserver variation analysis using virtual microscopy: a Multinational Study of the European Network for the Study of Adrenal Tumors (ENS@T). *Mod Pathol.* 2015;**28**(6):807-821.

28. Andrews KA, Ascher DB, Pires DEV, et al. Tumour risks and genotype-phenotype correlations associated with germline variants in succinate dehydrogenase subunit genes *SDHB*, *SDHC* and *SDHD*. *J Med Genet.* 2018;**55**(6):384-394.

29. Haller F, Moskalev EA, Faucz FR, et al. Aberrant DNA hypermethylation of SDHC: a novel mechanism of tumor development in Carney triad. *Endocr Relat Cancer.* 2014;**21**(4):567-577.

30. Vaz-Drago R, Custódio N, Carmo-Fonseca M. Deep intronic mutations and human disease. *Hum Genet.* 2017;**136**(9):1093-1111.

31. Else T, Marvin ML, Everett JN, et al. The clinical phenotype of SDHC-associated hereditary paraganglioma syndrome (PGL3). *J Clin Endocrinol Metab.* 2014;**99**(8):E1482-E1486.

32. Richter S, Klink B, Nacke B, et al. Epigenetic mutation of the succinate dehydrogenase C promoter in a patient with two paragangliomas. *J Clin Endocrinol Metab.* 2016;**101**(2):359-363.

33. Niemeijer ND, Papathomas TG, Korpershoek E, et al. Succinate dehydrogenase (SDH)-deficient pancreatic neuroendocrine tumor expands the SDH-related tumor spectrum. *J Clin Endocrinol Metab.* 2015;**100**(10):E1386-E1393.

34. Hansford S, Kaurah P, Li-Chang H, et al. Hereditary diffuse gastric cancer syndrome: *CDH1* mutations and beyond. *JAMA Oncol.* 2015;**1**(1):23-32.

35. Habano W, Sugai T, Nakamura S, et al. Reduced expression and loss of heterozygosity of the *SDHD* gene in colorectal and gastric cancer. *Oncol Rep.* 2003;**10**(5):1375-1380.

36. Whitworth J, Skytte AB, Sunde L, et al. Multilocus inherited neoplasia alleles syndrome: a case series and review. *JAMA Oncol.* 2016;**2**(3):373-379.

37. Bourdeau I, Grunenwald S, Burnichon N, et al. A SDHC founder mutation causes paragangliomas (PGLs) in the French Canadians: new insights on the SDHC-related PGL. *J Clin Endocrinol Metab.* 2016;**101**(12):4710-4718.

38. Bagnall RD, Ingles J, Dinger ME, et al. Whole genome sequencing improves outcomes of genetic testing in patients with hypertrophic cardiomyopathy. *J Am Coll Cardiol.* 2018;**72**(4):419-429.